

DOI:10.5937/jaes0-34344

Paper number: 20(2022)3, 1002, 971-977

www.engineeringsscience.rs \* ISSN 1451-4117 \* Vol.20, No 3, 2022

## INVESTIGATION OF RELATIVE INFLUENCE OF PROCESS VARIABLES IN A 10-KW DOWNDRAFT FIXED-BED GASIFIER WITH ANN MODELS

Hanif Furqon Hidayat, Rachman Setiawan, Radon Dhelika\*, Adi Surjosatyo, Hafif Dafiqurrohman

Department of Mechanical Engineering, Faculty of Engineering, Universitas Indonesia

\*radon@eng.ui.ac.id

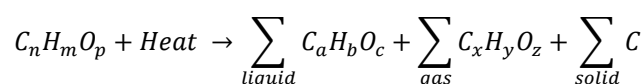
Biomass gasification is considered among promising solutions for renewable energy generation. The process converts the biomass, such as rice husk, to synthetic gas (syngas). It produces CO, CO<sub>2</sub>, CH<sub>4</sub>, and H<sub>2</sub> gas that are useful for internal combustion engines. The process is complicated to control. Hence, a thorough knowledge of this process is needed. One of the approaches to reveal the control parameters of the gasifier is using an artificial neural network (ANN). In this research, an ANN model is deployed from experiments that measure combustion temperature, intake, and discharge airflow rate as input variables. The output of this model is to predict the increase of combustion temperature in the reactor as this parameter is crucial for the design of an automated control system. From the two experiments, the models produce satisfying accuracy (R<sup>2</sup> = 0.832 and 0.911) and relatively low errors (RMSE values of 0.250 and 0.098). The neural network itself is used to analyze the significant control parameters by the permutation importance method.

Keywords: biomass gasification, artificial neural network, gasification temperature control

### 1 INTRODUCTION

One of the modern world challenges nowadays is the generation of sustainable and renewable energy to substitute fossil energy resources. In 2019, total global fossil fuel consumption was 136,761 TWh, with oil as the most consumed energy resources. In contrast, the total renewable energy consumption in 2019 was only 18,138 TWh, with conventional biofuels as the most used renewable energy resource. Biomass is considered as one of the promising renewable energy resources. The global potential of biomass is predicted to be approximately 150 EJ by 2035 that ranges from agriculture products, forestry, and organic waste [1]. Biomass may have a great potential to become a renewable and sustainable resource along with wind, solar, and hydropower energy. Although some rural areas already use biomass as their main energy resources, such as firewood and charcoal, the process of direct combustion is not yet efficient to be utilized for engines. There is a process called biomass gasification that converts feedstocks to synthetic gas or syngas, which could be burned in internal combustion engines (ICEs). There are three advantages to transform biomass to syngas, i.e. to increase the heating value of the fuel, remove sulphur and nitrogen that prevents releasing them into the atmosphere, and reduce the carbon-to-hydrogen (C/H) mass ratio in the fuel [2]. A gasification process involves four different steps in a gasifier reactor. The first step is drying, in which the moisture content of the feedstocks is reduced by heating the feedstocks to 100 °C, which would lose the water bound. The drying process will follow until the temperature reaches 200 °C, which removes the water irreversibly. The next stage is pyrolysis, which involves the thermal breakdown of hydrocarbon molecules of feedstocks into smaller gas molecules. This process forms tar that is considered as a side product of the syngas. There is one method for tar reduction that involves higher temperature called thermal cracking [3]. This method requires a higher temperature (>1100 °C) by adding external heating or internal heat generation. The third step is the combustion or oxidation, which burns the feedstocks and some of the produced synthetic gas from pyrolysis and becomes the heat source for the rest of the reactor zones [4]. Then, the final stage is the reduction, which produces a large amount of synthetic gas that consists of CO, CO<sub>2</sub>, CH<sub>4</sub>, and H<sub>2</sub>[2].

Pyrolysis reaction [2]:



Combustion reaction [2]:  $C + O_2 \rightarrow CO_2$

Gasification of carbon [2]:  $C + 1/2O_2 \rightarrow CO$

Methanation reaction[2]:  $C + 2H_2 \rightarrow CH_4$

Syngas production reaction [2]:  $CH_4 + H_2O(catalyst) \rightarrow CO + 3H_2$

The process in a gasifier reactor needs advanced modelling to understand the whole reactions involved. Some advancements have been made in numerical modelling methods recently that helps a better understanding of the process inside the gasifier reactor. At least there have been four approaches developed in recent years [5], [6]. The

first method is thermodynamics equilibrium modelling, which involves Gibbs free energy equations [7], [8]. This approach is useful to model any gasifier type and its operational conditions in different operating parameters. Although relatively easy to apply to study the control parameter of the gasifier reactor, this approach has some limitations, especially its inability to describe stationary gasification reactions and detailed processes. The second approach is kinetic modelling, which solves the thermodynamic equilibrium approach limitation to correlate between gasifier design parameters and produced gas composition [9]–[11]. This method involves some parameters such as reaction rate, residence time, reactor hydrodynamics, and reactor length [12]. It also has some advantages as compared to other approach, such as its accuracy in the analysis of gasification reactions that are useful for developing the gasifier design. However, kinetic modelling is not practical to control the gasifier online and highly dependent on the design of the gasifier. The third method is computational fluid dynamics (CFD), which is the most advanced approach to analyze the gasification process extensively [13], [14]. CFD simulation could produce the profile of temperature, solid-gas phase state, and the complete analysis of chemical and mechanical fluid properties of the bed. Although its superior in terms of the completeness of the analysis, CFD needs powerful resources to accomplish the computation. Also, it does not produce a practical analysis to control the parameters of the gasifier. The last method is artificial intelligence, which could model linear and non-linear problems [15], [16]. Artificial neural network (ANN) is one of the most used methods to model desired output from certain controlled parameters. In general applications, ANN is commonly used to predict the output from known input variables, either for classification or regression purposes [17]–[19]. Several authors had utilized ANN to predict and analyze the gasifier performance from previous experimental data. Compared to previous approaches mentioned before, ANN shows a better analysis in its accuracy. Also, ANN could show the weight values from each variable that help to decide which parameter has more impact on the output [20]. In this study, the ANN model was deployed to analyze the impact of operational parameters that consist of air intake flow, air outtake flow, biomass feed rate, and ash removal rate on the temperature progression in the reactor. The data are obtained from the previous experiments of a fixed-bed downdraft gasifier [21]. Since this study is preliminary research, the goal of the ANN model is to predict the temperature progression in a fixed-bed gasifier reactor and decide which parameter has more impact on controlling the temperature. The prediction generated from the model will be verified in the experiment for validation and feedback on PLC designing for future automation purposes. There is a more advanced neural network approach called recurrent neural network (RNN) that could analyze time-series data better. However, the experimental data of this study is insufficient to be modeled in an RNN. The results of this study would be advanced as feedback for the following research which will utilize RNN models.

## 2 METHODS

### 2.1 Gasifier setup and the data logging

The gasifier used in this work is the second prototype of a downdraft fixed-bed gasifier developed in our group, which incorporates improvements from the previous prototype [22][23]. Figure 1 shows the schematic of the gasifier. In the second prototype, the total installed capacity is 10 kW, and it is equipped with AC motors at various locations. The actuators aimed to control the temperature of the reactor in its ideal range. Table 1 shows the temperature range of the reactor in different zones.

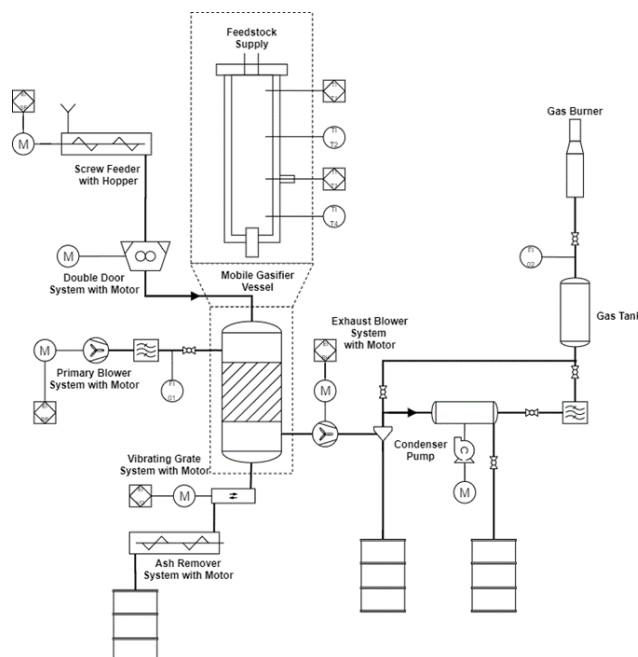


Fig. 1: Schematic of the 10 kW gasifier system used in this experiment

Table 1: Temperature range of each zone in the gasifier reactor

Reactor Zone	Temperature (°C)
Drying zone	100-200
Pyrolysis zone	200-700
Combustion zone	700-1000
Reduction zone	500-600

Table 2: Properties of the rice husk used in this study

Parameter	Unit	Result	Method
<b>Proximate:</b>			
Moisture in Analysis	%, adb	8.6	ASTM D 3173
Ash Content	%, adb	20.5	ASTM D 3174
Volatile Matter	%, adb	57.6	ISO 562-2010
Fixed Carbon	%, adb	13.3	ASTM D 3172
<b>Ultimate:</b>			
Carbon (C)	%, adb	35.52	ASTM D 5373
Hydrogen (H)	%, adb	5.8	ASTM D 5374
Nitrogen (N)	%, adb	0.5	ASTM D 5375
Oxygen (O)	%, adb	37.6	ASTM D 5376

The experimental runs were conducted two times with a feedstock of rice husk. The first run was conducted for around 25 minutes, and the second one was around 40 minutes. The logged data was the temperature of combustion and the frequency of AC motors at three different locations: the primary air blower system, the discharge blower system, and the vibrating grate system. The three types of data from the AC motors are intended to represent the flow rate of the air entering the reactor, the flowrate of the generated syngas exiting the reactor, and the removal rate of the feedstock, respectively. The data was logged every two seconds. During this preliminary experimental run of the gasifier, the feedstock was fed manually to the reactor. Hence, the motors at the screw feeder and the double door were operated at a constant rate. The feeding rate is assumed constant for the analysis in the later section of this work.

## 2.2 Modelling of neural network

The steps in the modelling of the neural network are shown in the flowchart in Figure 2.

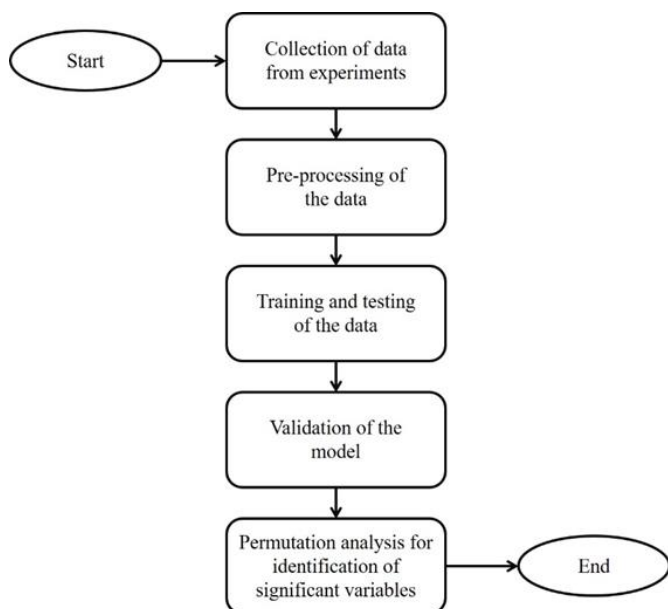


Fig. 2: Flow chart of the steps in model development

After collecting the data from the experiments, the subsequent step was the pre-processing. In this step, the data was carefully selected when the combustion temperature has reached 550 °C. Then, the selected data for the output variable was converted to the difference between the previous data with the next data, i.e. the difference of combustion temperature between  $n$  and  $(n+2)$  second. This approach was taken because the output variable of temperature difference which is processed by the neural network will be scaled from -1 to 1. Table 2 below summarizes the input and output variables used for the modelling of the neural network.

The neural network model was generated from a Python library named Keras. Table 3 shows the structure of the neural network built on Keras API. The optimizer used in the model is RMSPROP which is more suitable to the dataset than ADAM. Concurrently, the loss function optimized in the model is mean squared error which is the correct option for the regression model. The neuron details are obtained from trial-and-error process.

Table 3. Input and output variables of the neural network

Input variables	Output variables
Frequency at primary blower	Difference of combustion temperature between n and (n+2) second
Frequency at exhaust blower	
Frequency at vibrating grate	
Combustion temperature at n second	

Table 4 Details of the neural network model

Particulars	Specifications
Network type	Feed forward backpropagation
Optimizer	RMSPROP
Loss function	Mean squared error
Kernel regularizer	0.01
Number of input layer unit	4
Number of output layer unit	1
Number of hidden layers	3 (number of neurons respectively: 8, 4, 4)
Number of epochs	1000

Subsequently, training and testing of the data were conducted. The measure of loss during the process was the MSE (mean-square error), using equation (1). Validation was carried out by summing cumulatively the initial temperature with the increment obtained from the prediction and then to compare it with the experimental data. The  $R_2$ , using equation (2) was then obtained.

$$RMSE = \sqrt{\frac{1}{N} \sum_{i=1}^N (\text{experimental}_i - \text{model}_i)^2} \quad (1)$$

$$R^2 = 1 - \frac{\sum_{i=1}^N (\text{experimental}_i - \text{model}_i)^2}{\sum_{i=1}^N (\text{model}_i)^2} \quad (2)$$

The final step of the process was the permutation analysis of features. This method is a technique for model inspection that enables the identification of relative influence of input variables on model outputs. The method, which partitions the connection weights between features and the target, is based on the formula which is shown in equation (3) [23].

$$i_j = s - \frac{1}{K} \sum_{k=1}^K s_{kj} \quad (3)$$

In this method, values of each variable are randomized and would result in changes in the scoring of the model. A decline of the scoring can be inferred as an indication of how important the tested variable to the model. The higher the scoring of the weight, the more the model is dependent to the tested variable.

### 3 RESULTS AND DISCUSSION

The data of combustion temperature from the first and second experimental run are shown in Figure 3. Additionally, Figure 4 shows the frequency data of the AC motors of the primary blower, exhaust blower, and vibrating grate, as explained in the previous section.

Based on the set of data shown in Figure 3 and 4, the models were then developed. Subsequently, the models were utilized to predict the combustion temperature. The predicted results are shown in Figure 5, which is already combined with the experimental data. The  $R^2$  values obtained were 0.832 and 0.9114 for the first and second set of data, respectively. In addition, the RMSE values are 0.2497 and 0.0978, which can be considered acceptable from previous research (ranging from 0.3421 to 1.2685) [24].

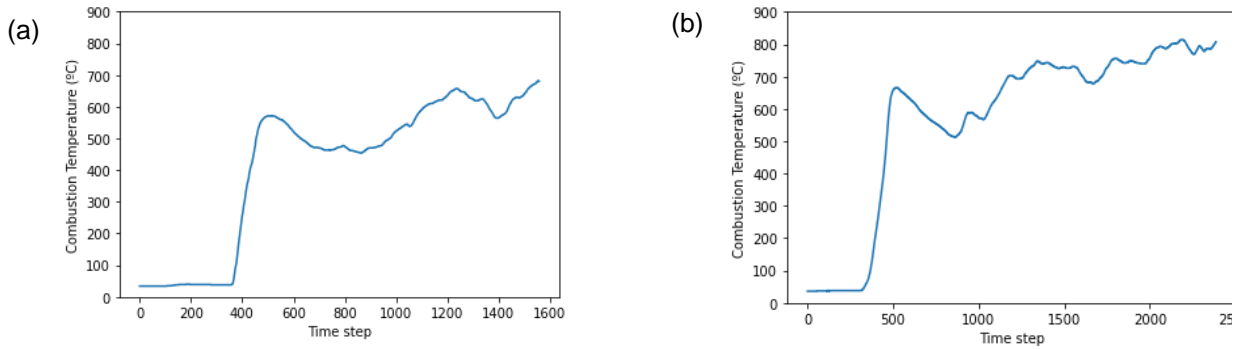


Figure 3. Combustion temperature of (a) first and (b) second experimental run

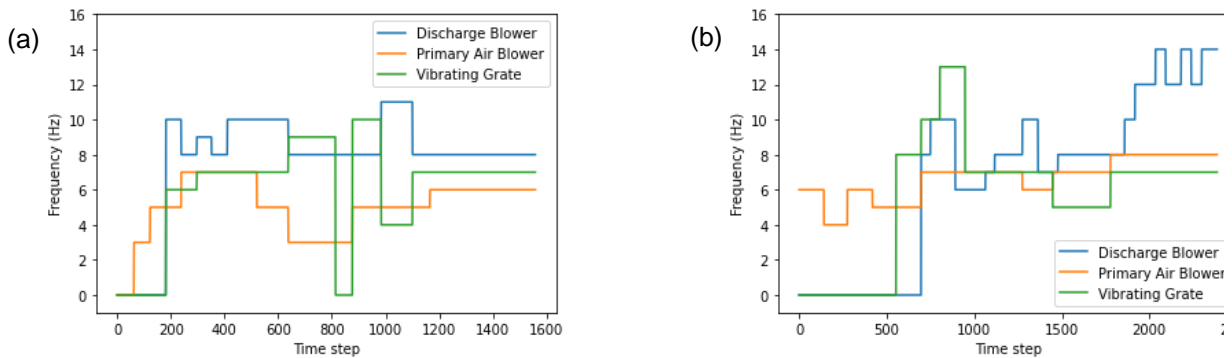


Figure 4. Motors' frequencies for discharge blower, primary air blower, and vibrating grate (a) first and (b) second experimental run

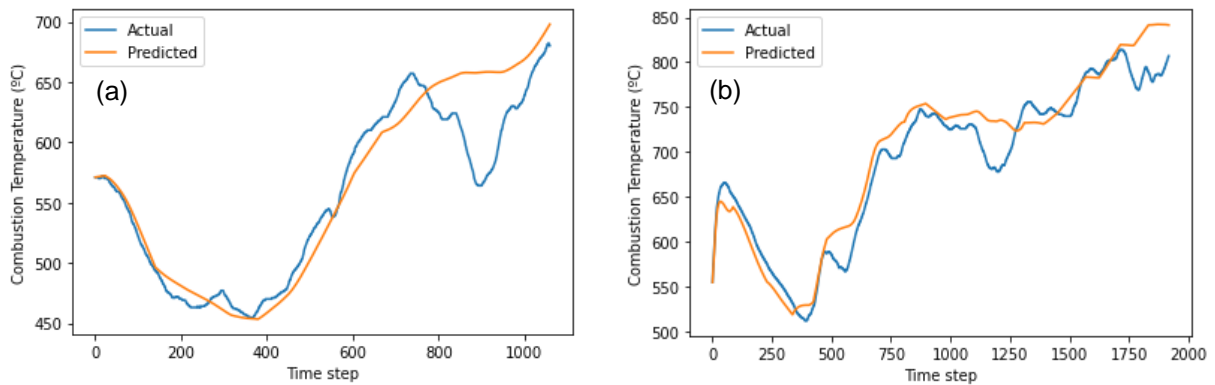


Figure 5. Comparison between experimental data and data predicted by the ANN models for (a) the first experimental run and (b) the second experimental run

The following step was the permutation analysis whose results are shown in Table 4.

Table 5. The produced weight from ANN process in the gasifier\

Weight	Feature
0.0306 ± 0.0074	Vibrating Grate
0.0244 ± 0.0049	Primary Blower
0.0160 ± 0.0060	Discharge Blower
0.0133 ± 0.0031	Combustion Temp
0.0317 ± 0.0048	Combustion Temp
0.0289 ± 0.0048	Vibrating Grate
0.0197 ± 0.0055	Primary Blower
0.0130 ± 0.0016	Discharge Blower



The results above show the importance of each feature from the neural network. Based on the two-model comparison, the produced weight from permutation importance is relatively identical other than the combustion temperature feature. From the first model, the combustion temperature feature has the least important than the other features. Meanwhile, the second model shows that the combustion temperature is the most significant feature. This condition is likely caused by greater temperature anomaly from the first experiment. Since the results show an opposite trend to one another, the combustion temperature feature is excluded from the analysis.

Meanwhile, the other three features could produce the analysis better due to their consistency in values. First, the vibrating grate that controls the ash removal rate affects the flow of the biomass at the upper part of the reactor. The grate indirectly involves the change of temperature. When the ash removal rate is higher, the combustion temperature tends to equal the upper zone temperature. This feature might be the most important feature than the primary blower and discharge blower feature. Second, the primary blower controls the air supply rate to combust the biomass inside the reactor. When the air supply increases, the biomass would burn easier, so it would increase the combustion temperature. However, the increase of the temperature depends on the heating value of the biomass. Third, the discharge blower controls the discharge rate of the syngas. Additionally, it triggers heat transfer to lower zones. Hence, the rise of the discharge rate affects the temperature at the lower zones. Yet, it depends on the biomass heating value inside the reactor as it is known by the gas composition in the process.

There are some issues that lead to the inconsistency of the prediction results:

- Ideally, the frequency of motors is always linear to the airflow. However, the condition of blowers deteriorates gradually after several runs because the airflow is lower than previous runs at the exact frequency of the motor. This condition happens due to gasification residues accumulating throughout the piping system and restricting the airflow. For more accurate data acquisition of the airflow, flowmeters should be installed at the outlet of each blower.
- Biomass feeding rate is assumed constant in this study. Although, the feeding mechanism is operated manually hence the rate varies. The gasifier setup has a regulated feeding rate mechanism using a screw controlled by a variable motor. However, the rice husk often clogs the screw and trips the motor due to poor design.

#### 4 CONCLUSIONS

In this investigation, ANN model is used to predict temperature that occurs in the reactor of a downdraft biomass gasifier that is related to the regulators, producing synthetic gas continuously. The result revealed that the value of  $R^2$  is obtained by 0.9114 when the RMSE is 0.0978, thus the neural network model showed that the temperature value in the second experiment is almost similar.

Furthermore, the most significant feature in the downdraft gasifier system is the vibrating grate that controls the bed to remove the ash from the reactor and this feature has plenty of effects on the temperature distributions with the produced weights of  $0.0306 \pm 0.0074$  and  $0.0289 \pm 0.0048$  for the first and second model, respectively. However, further study should be conducted which involves more data from more experimental runs. Additionally, other parameters are also needed, such as real-time gas composition and adding air flow rate measurement to constitute the exact operational condition.

#### 5 ACKNOWLEDGEMENT

This work was funded by HIBAH PUTI Q3 fiscal year 2020 (NKB 2013/UN2.RST/KP.05.00/ 2020).

#### 6 REFERENCES

- [1] BP, "Statistical Review of World Energy, 2020 | 69th Edition," Bp, vol. 69, 2020.
- [2] P. Basu, Biomass gasification, pyrolysis and torrefaction: Practical design and theory. 2018. doi: 10.1016/C2016-0-04056-1.
- [3] S. Anis and Z. A. Zainal, "Tar reduction in biomass producer gas via mechanical, catalytic and thermal methods: A review," Renewable and Sustainable Energy Reviews, vol. 15, no. 5. 2011. doi: 10.1016/j.rser.2011.02.018.
- [4] B. M. Jenkins, L. L. Baxter, and J. Koppejan, "Biomass Combustion," in Thermochemical Processing of Biomass, 2019. doi: 10.1002/9781119417637.ch3.
- [5] A. Ramos, E. Monteiro, and A. Rouboa, "Numerical approaches and comprehensive models for gasification process: A review," Renewable and Sustainable Energy Reviews, vol. 110. 2019. doi: 10.1016/j.rser.2019.04.048.
- [6] D. Baruah, D. C. Baruah, and M. K. Hazarika, "Artificial neural network based modeling of biomass gasification in fixed bed downdraft gasifiers," Biomass and Bioenergy, vol. 98, 2017, doi: 10.1016/j.biombioe.2017.01.029.

- [7] M. Puig-Arnavat, J. C. Bruno, and A. Coronas, "Modified thermodynamic equilibrium model for biomass gasification: A study of the influence of operating conditions," *Energy and Fuels*, vol. 26, no. 2, 2012, doi: 10.1021/ef2019462.
- [8] H. J. Huang and S. Ramaswamy, "Modeling biomass gasification using thermodynamic equilibrium approach," in *Applied Biochemistry and Biotechnology*, 2009, vol. 154, no. 1–3. doi: 10.1007/s12010-008-8483-x.
- [9] I. Adeyemi and I. Janajreh, "Modeling of the entrained flow gasification: Kinetics-based ASPEN Plus model," *Renewable Energy*, vol. 82, 2015, doi: 10.1016/j.renene.2014.10.073.
- [10] S. Halama and H. Spliethoff, "Reaction Kinetics of Pressurized Entrained Flow Coal Gasification: Computational Fluid Dynamics Simulation of a 5MW Siemens Test Gasifier," *Journal of Energy Resources Technology*, vol. 138, no. 4, 2016, doi: 10.1115/1.4032620.
- [11] A. Gagliano, F. Nocera, F. Patania, M. Bruno, and D. G. Castaldo, "A robust numerical model for characterizing the syngas composition in a downdraft gasification process," *Comptes Rendus Chimie*, vol. 19, no. 4, 2016, doi: 10.1016/j.crci.2015.09.019.
- [12] R. Wu, J. Beutler, and L. L. Baxter, "Non-catalytic ash effect on char reactivity," *Applied Energy*, vol. 260, 2020, doi: 10.1016/j.apenergy.2019.114358.
- [13] Q. Xue and R. O. Fox, "Multi-fluid CFD modeling of biomass gasification in polydisperse fluidized-bed gasifiers," *Powder Technology*, vol. 254, 2014, doi: 10.1016/j.powtec.2014.01.025.
- [14] A. Klimanek, W. Adamczyk, A. Katelbach-Woźniak, G. Węcel, and A. Szlęk, "Towards a hybrid Eulerian-Lagrangian CFD modeling of coal gasification in a circulating fluidized bed reactor," *Fuel*, vol. 152, 2015, doi: 10.1016/j.fuel.2014.10.058.
- [15] V. Arcotumapathy, F. Alenazey, and A. A. Adesina, "Artificial neural network modeling of forced cycling operation between propane steam reforming and CO<sub>2</sub> carbon gasifier," in *Catalysis Today*, 2011, vol. 164, no. 1. doi: 10.1016/j.cattod.2010.12.027.
- [16] M. Puig-Arnavat, J. A. Hernández, J. C. Bruno, and A. Coronas, "Artificial neural network models for biomass gasification in fluidized bed gasifiers," *Biomass and Bioenergy*, vol. 49, 2013, doi: 10.1016/j.biombioe.2012.12.012.
- [17] H. Wang, D. Chaffart, and L. A. Ricardez-Sandoval, "Modelling and optimization of a pilot-scale entrained-flow gasifier using artificial neural networks," *Energy*, vol. 188, 2019, doi: 10.1016/j.energy.2019.116076.
- [18] M. Ozonoh, B. O. Oboirien, A. Higginson, and M. O. Daramola, "Performance evaluation of gasification system efficiency using artificial neural network," *Renewable Energy*, vol. 145, 2020, doi: 10.1016/j.renene.2019.07.136.
- [19] A. Y. Mutlu and O. Yucel, "An artificial intelligence based approach to predicting syngas composition for downdraft biomass gasification," *Energy*, vol. 165, 2018, doi: 10.1016/j.energy.2018.09.131.
- [20] R. Mikulandrić, D. Lončar, D. Böhning, R. Böhme, and M. Beckmann, "Artificial neural network modelling approach for a biomass gasification process in fixed bed gasifiers," *Energy Conversion and Management*, vol. 87, 2014, doi: 10.1016/j.enconman.2014.03.036.
- [21] R. Setiawan, H. F. Hidayat, H. Dafiqurrohman, A. Surjosatyo, and R. Dhelika, "Performance Evaluation of a Continuous Downdraft Gasification Reactor Driven by Electric Motors with Manual Mode of Operation," *Journal of Engineering and Technological Sciences*, 2021. (Accepted)
- [22] L. Andromeda, A. Surjosatyo, H. Dafiqurrohman, and M. H. Amirullah, "Analysis of fix bed downdraft biomass gasification reactors continues operating characteristics towards synthetic gas quality," in *AIP Conference Proceedings*, 2020, vol. 2255. doi: 10.1063/5.0013681.
- [23] I. R. Kurnianto, A. G. Setiawan, A. Surjosatyo, H. Dafiqurrohman, and R. Dhelika, "Design and Implementation of a Real-Time Monitoring System Based on Internet of Things in a 10-kW Downdraft Gasifier," *Evergreen*, vol. 9, no. 1, pp. 145–149, Mar. 2022, doi: 10.5109/4774230.
- [24] F. Pedregosa et al., "Scikit-learn: Machine learning in Python," *Journal of Machine Learning Research*, vol. 12, 2011.
- [25] F. Elmaz and Ö. Yücel, "Data-driven identification and model predictive control of biomass gasification process for maximum energy production," *Energy*, vol. 195, 2020, doi: 10.1016/j.energy.2020.117037.

*Paper submitted: 09.10.2021.*

*Paper accepted: 27.12.2021.*

*This is an open access article distributed under the CC BY 4.0 terms and conditions.*